

# Application of finite element method to an overhead crane bridge

CAMELIA BRETOTEAN PINCA, GELU OVIDIU TIRIAN, ANA JOSAN

Department of Mechanical Engineering and Management

“Politehnica” University of Timisoara

Revolutiei str., no. 5, Hunedoara

ROMANIA

camelia.bretotean@fih.upt.ro, ovidiu.tirian@fih.upt.ro, ana.josan @fih.upt.ro

**Abstract:** This paperwork analyses the tension and deformation state of the resistance structure of an overhead crane bridge which used for all the processes performed in the hall of a continuous casting department of an iron and steel plant in order to find out the best sizes. This analysis is made up with the help of the COSMOS software who enables us to make evolved finite items – shell-type with three or four nodes per element. The shell-type finite items belong to the  $C^1$ -class items, and they have a field variable and the I-type derivatives working continuously alongside the frontier, meanwhile the II-type continuous derivatives per item are not continuous alongside the frontier. These finite items allow us to design some complex structures more accurately, such as the resistance structure of the crane bridge. This example is not intended to be the only solution when designing similar structures, but the authors of this paperwork believe that it is providing enough information and useful solutions for the analysis of the tension and deformation state in case of finite items.

**Key-Words:** crane bridge, analysis, model, resistance, overhead, finite elements, shell.

## 1 Introduction

Most of the time, the resistance structures who have not been statically determined, cut to the right sized, and checked out by the classic methods of the material strength cause the oversizing, because specialists use approximate measurements in order to decrease the number of mathematical calculation. Modern methods who use automatic data processing allow us to study the tension more accurately, especially due to the operative method of balance and continuity equation calculation, [4],[6],[11]. As far as the validity of the accuracy and operative method is concerned, they are real is the shaping up of the structure and the connection means are as good as possible [4],[6],[11]. This paperwork analyses the tension and deformation state of the resistance structure of a crane bridge who is used for all the processes performed in the hall of a continuous casting department of an iron and steel plant. This analysis is made with the help of the old method used for producing finite items and the COSMOS calculation software, [14], [16]. The results we have obtained allow us to produce a complete study about the tension and deformation state of the resistance structure of a crane bridge, and to highlight all details based on the operation forces. Based on those results, we are able to produce some details about the lack of resilience of

the resistance structure, and to make some decisions about how to improve the bearing capacity of the equipment, and, if there is the case, we are able to perform the best size optimization, [9]. This is possible only if we do not exceed the limits of the acknowledged resistance, in order to redesign the resistance structure of the crane bridge, meanwhile the material consumption is highly reduced.

## 2 The description of the resistance structure component

The resistance structure is made of two longitudinal beams - I and II, as well as two end beams: left and right, which make up a dark plane contour. The longitudinal beams have a variable section at their ends, fig.1 and the end beams have a constant section alongside their lengths, fig.2. The cross section of the resistance elements – caissons – is symmetrical and made of universal iron – they are weld together, fig.3.

The cross-sections of the resistance elements are made of two side cores who are 6 mm thick, and two tracks – one high and one low – who are 8 mm thick. The connection between the cores and the tracks is provided by the welding lines, because these beams are stressed repeatedly and that may

The forces that stress the resistance structure are perpendicular on the structure plane and they make up a space system. The global analysis of the resistance structure has been performed for the best positions, as well as for the less favourable positions of all the forces.

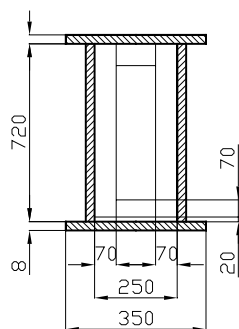


Fig.3 The cross section of the resistance elements

Thus, the calculation is more precise if the finite elements are more accurate and thus, the resistance structure is more appropriate. Due to the complex structure of the resistance we have analyzed, it is difficult to choose the type of the finite element who we should use for producing a discrete item; and it

is related to the way we are able to provide the continuous process amongst the elements. A more accurate analysis needs to use the finite items who are able to approximate the resistance structure as accurate as possible.

The evolved calculation software use evolved finite elements, such as shell-type thin plates, [4], [6], [10], [14], [16].

This type of finite elements do not allow the most appropriate amount of release, except for the shifting values of the nodes we use for demonstrate the elasticity theory we use for the analytical calculation, [4], [10], [11].

Fig.4 describes the shell-type finite element with three nodes, who needs extra release degrees, besides the liniary shifting  $w(x,y)$ , according to the direction of the  $z$ -normal on the median line of the plate and the angular shifting  $\varphi_x = \frac{\partial w}{\partial x}$  and

$\varphi_y = \frac{\partial w}{\partial y}$  - using the carthesian axis system  $xyz$ .

They refer to the two-type derivatives of the shifting  $w(x,y)$ ,  $(\frac{\partial^2 w}{\partial x^2}; \frac{\partial^2 w}{\partial y^2}; \frac{\partial^2 w}{\partial x \partial y})$ . In this case, if we

refer to the surface of the elements, we can register some discontinuous twisting and bending when being shaped up. If we must use the curved element, it works continuously, and that is not consistent [12], [16].

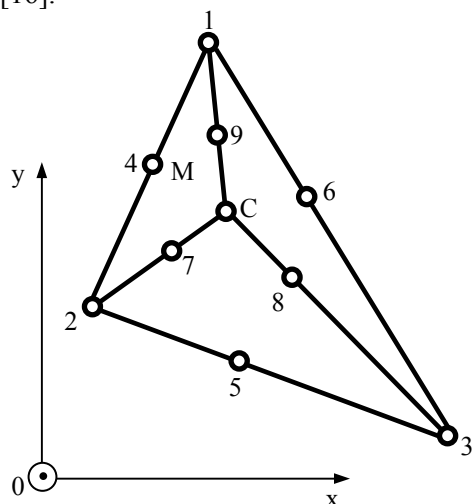


Fig.4 Evolved finite element of shell type thin plate - triangular finite element;

Clough and Tocher have come up with the solution for providing the compatibility amongst the elements – for the thin plate-type finite element with three nodes. Clough and Felippa have provided the solution for the four nodes-type, [4],[6],[11]. These

elements have different release degrees – shifting and node turning – and they have been considered only if any physical deformation might occur. Besides the rotations -  $\varphi_x = \frac{\partial w}{\partial x}$  and

$\varphi_y = \frac{\partial w}{\partial y}$ , Clough and Tocher have come up with

some release degree for the node turning -

$\varphi_n = \frac{\partial w}{\partial n}$ , where „n” represents the appropriate

value of the median line of the plate surface, [4], [6], [11]. In case of the finite elements shaping up – shell-type, the compatibility amongst the elements could be provided by the complete cubic polynomial, according to the relation (1), [6],[11]:

$$w(x,z) = c_1 + c_2x + c_3y + c_4x^2 + c_5xy + c_6y^2 + c_7x^3 + c_8x^2y + c_9xy^2 + c_{10}y^3 \quad (1)$$

Where:  $c_1, \dots, c_{10}$  – generalized release degrees of the element who ensures the compatibility amongst elements.

Because  $w$ -shifting, who has  $\varphi_x = \frac{\partial w}{\partial x}$ ;

$\varphi_y = \frac{\partial w}{\partial y}$  and  $\varphi_n = \frac{\partial w}{\partial n}$ , leads with 12 release

degree on the triangular element with three nodes, we have created some macro-elements made of three sub-triangles, fig.4. They are connected to the common node C, which is situated in the central point of the element. For such elements, specialists have used additonal nodes – from 4 to 9, who are situated in the middle of all sides, fig. 4. Therefore, if we use a complete cubical polynomial, such as the one presented in relation (1), we have „30” generalized release degrees. In order to establish them, we use the following margin terms:

-  $w$ -shifting nodal values:  $\varphi_x = \frac{\partial w}{\partial x}$  and

$\varphi_y = \frac{\partial w}{\partial y}$ , considering that each node is connected

to two sub-angles. The total number is: 3 nodes x 3 terms/node x 2 common node elements = 18 margin terms;

- normal turning  $\varphi_n = \frac{\partial w}{\partial n}$  from intermediary nodes

4, 5 and 6, who generate the following margin terms: 1node x 3 terms /node = 3 margin terms;

- continuous  $w$ -shifting within the inner node - „M”, considering that this node is connected to three sub-triangles, who generate the following margins

terms: 1 node x 3 terms /node x 3 common elements for each node = 9 margin terms.

In such a case, we have „30” equations with „30” unknown elements, who allow us to establish the approximative functions enabled by the explicite relation (1). According to fig.5 , the number of release degrees is „12”. These nodes are represented by the normal slope amongst the intermediary nodes, the w-shifting, and  $\varphi_x$ ,  $\varphi_y$  of the top nodes. This type of element is called LCCT-12 (Linear Curvature Compatible Triangle) and it ensures the compatibility amongst elements, but it is enabled by the intermediary nodes situated in the middle of all sides. By using terms, such as the curve variation, who should be linear along the appropriate side, we are able to eliminate the intermediary nodes of that side. Thus, the curve of the intermediary node reaches the value of the arithmetical mean of all curves who define the side. By eliminating one node at a time, we get the other Clough-Tocher finite elements: LCCT-11, LCCT-10 and LCCT-9, [4], [6],[11].

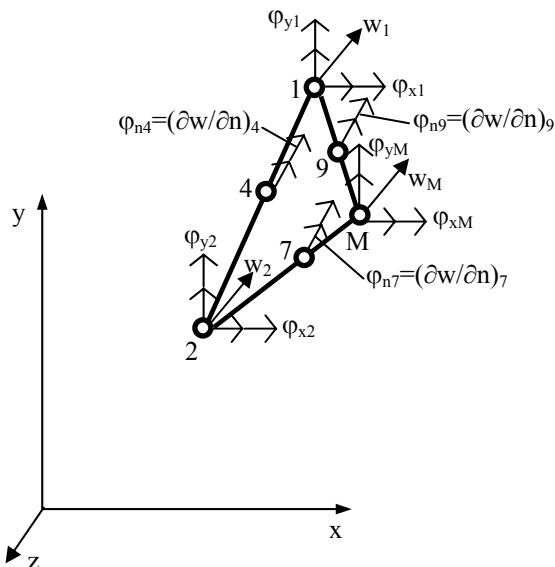


Fig.5 Evolved finite element of shell type thin plate – release degree presentation

Using LCCT-11-type Clough-Tocher element, Clough-Felippa establish the quadrilateral element Q12, obtained by assembling four finite elements - LCCT-11, by static condensing which enables us eliminate the release degrees corresponding to the inner nodes, fig. 6.

This finite element has 12 release degrees – 3 release degrees for each node – represented by the  $w(x,y)$  shifting and the  $\varphi_x$  and  $\varphi_y$  rotations.

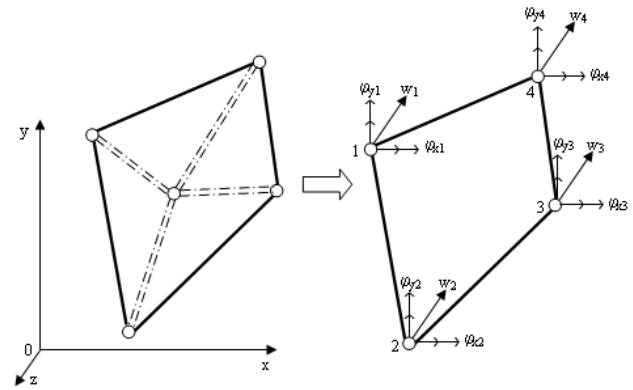


Fig.6 Quadrilateral finite element - Q 12

Nowadays analysis software based on finite elements enclose such evolved finite elements who are able to ensure the compatibility amongst all elements for each stress case. COSMOS calculation software uses finite elements – one finite element is called shell and it has three or four nodes/element. COSMOS software uses such finite elements, and they help the software to shape up the resistance structures of any metallurgical equipment. We could neglect any deformation caused by the cutting forces. The numbers of the nodes are allowed both in a trigonometrical way, and the other way around. Fig. 7 describes the local axis system -  $xyz$  - and the finite element is considered to shape up the equipments.

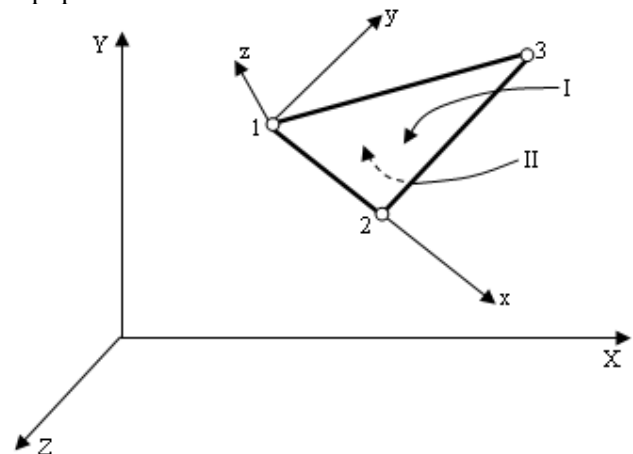


Fig.7 Representation of the shell-type finite element for the local coordinates axis system

In fig. 7- XYZ represents the global axis system; xzy represents the local coordinate system of the element, and I and II are those sides we can use for performing weight and contours, [11]. We see that the coordinates local system of the element has the „x” axis oriented upwards, from the first to the second node; the „y” axis is composed in the plan of the element, and it is perpendicular on the „x”

axis, and oriented towards the third node; the „z” axis makes the right cartesian system complete.

In this study finite element modeling is carried out by means of the COSMOS package, in the finite elements library which secure a very good calculation accuracy, with deviations under 4 % related to the exact methods of calculation, [4] [5], [6], [11], [16]. The availabilities provided by the pack of programmers COSMOS/M, which don't limit the analysis dimension by the number of elements or the number of nodes used, [4], [6], [11]. This type of finite elements allows us to perform a linear or non-linear analysis of the resistance structure of the crane bridge.

#### 4 The modelling of the strength structure

For shaping up the resistance structure, we have followed the next stages:

- enabling the geometrical shaping up of the structure and the discretization for a finite number of structure elements, who is characterized by the shape and the size of the cross-section, and the lengths and orientation of the axis;
- establishing the position of the connection nodes using all co-ordinates, in order to enable the connection amongst the structural elements and rail nodes;
- designing the connection amongst the structural elements and the outer connections, complying with the non-deformation condition (geometrically speaking) of the resistance structure and the invariable law based on leaning basis;
- designing the material behaviour of the resistance structure, according to the characteristic curve, described by both the tension relation ( $\sigma$ ) and deformation ( $\epsilon$ ), and force ( $F$ ) and shifting ( $u$ );
- designing all actions considering the way they work, the distribution along the resistance structure, their evolution in due time, as well as their specific use conditions; thus, we are able to define the calculation features of each action: intensity, use (focused or distributed; static or mobile), and the features of the action (static or dynamic).

In order to prepair the input data boxes, according to the previous stages, we have performed it according to the requirements of the COSMOS calculation software, for the crane bridge we study. Because the geometrical model has been elaborated in accordance with the workshop drawings, and the height number of elements of shell type used at meshing has allowed a calculation model very closed to the real geometry of the strength structure

of the analyzed crane bridge. In modelling with COSMOS software was used Youngs modulus ( $E$ )  $2,1 \times 10^5 \text{ N mm}^2$  and the Poisson ratio ( $\nu$ ) 0,3 for finite element analysis [4], [6],[13],[15] :

The boundary conditions regarding the supporting and loading way have been introduced as follows, [3], [6], [8], [11], [13]:

a. In the insert of blockings for certain degrees of freedom from the structure nodes, we had in view the presence of those four wheels of the crane bridge. For the nodes placed at the drive wheels level there have been introduced blockings for the linear displacements  $u$ ,  $v$  and  $w$  according to the three directions of the global system of axes XYZ of the structure, and for the driven wheels there have been introduced only the linear blocking  $u$  and  $w$  according to the directions  $y$  and  $z$ .

b. The forces have been distributed in the nodes in front of their application area according to the loading diagram of the crane bridge. The existence of some eccentric loadings by means of some rigid arms, has led to their replacement with an equivalent system of loads directly applied on the structure, in order to avoid the supplementary use of some finite elements of beam type with high stiffening.

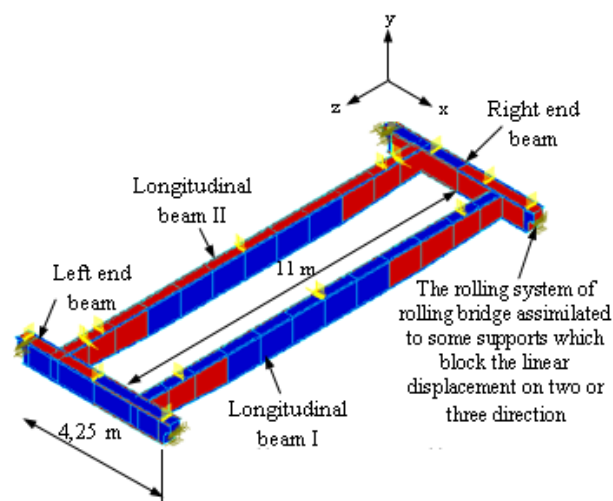


Fig.8 Solid model of the resistance structure

In order to design the shape of the resistance structure we have used two reference systems: a global reference system that we report the entire problem to, and a local reference system which is associated to a sub-domain of the problem we are analyzing. When modeling, the difference amongst the aggregate, the loading and the weight of the elements is calculated in condensed mass. The solid model of the crane bridge is presented in fig.8.

Fig.9 describes the discrete resistance structure with shell-type finite elements in detail. The big

number of shell-type finite elements allowed us to come up with a calculation method which is almost similar to the real shape of the resistance structure we have analyzed.

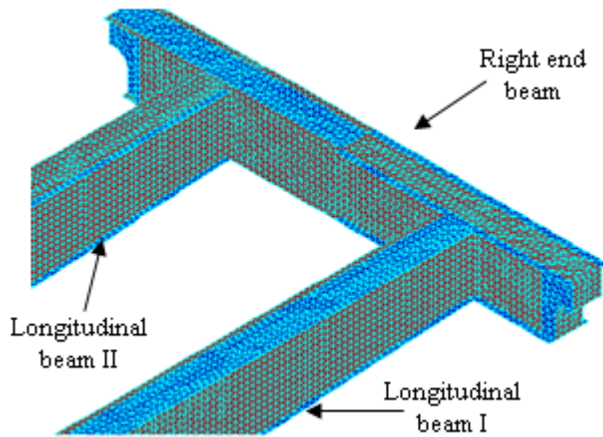


Fig.9 Discrete resistance structure of the crane bridge with shell-type finite element

The calculation method we have produced helped us make up a complete study about the tension and deformation state of the resistance structure of the crane bridge and to highlight the detail of the focusing and the division of the tensions, as well as of their deformations caused by the working forces.

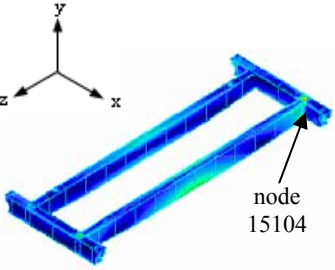
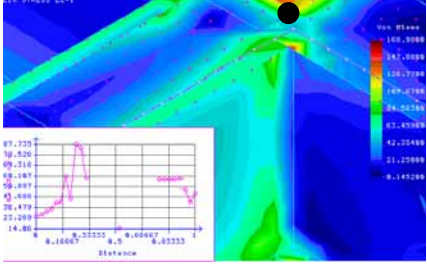
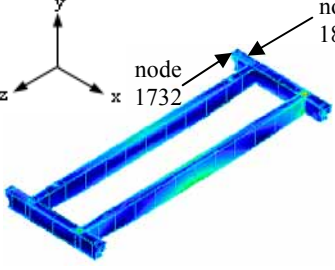
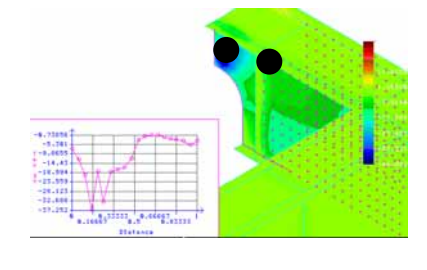
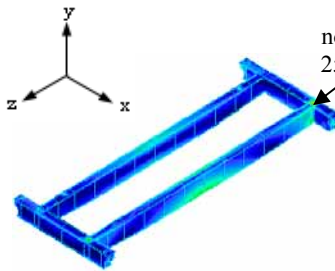
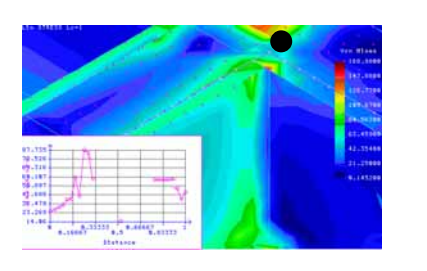
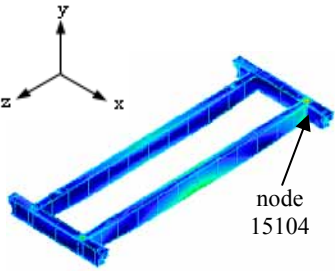
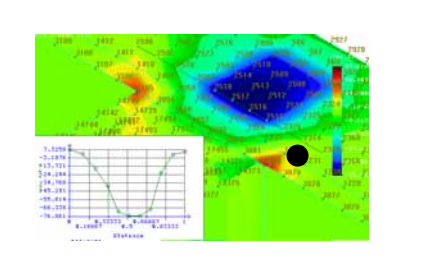
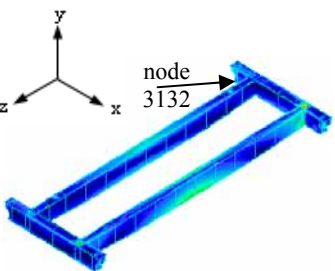
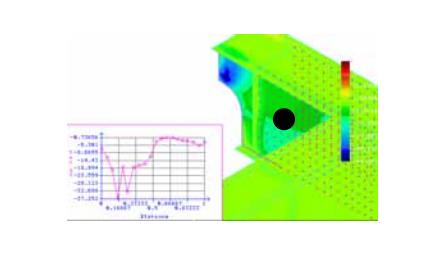
## 5 Results

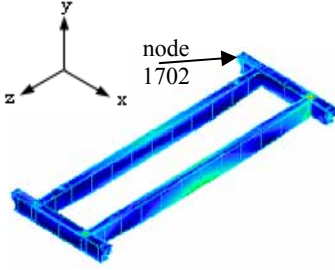
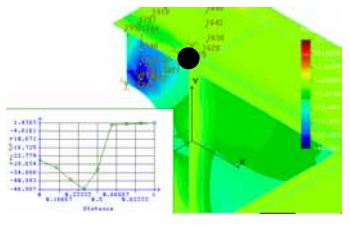
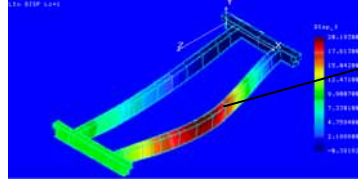
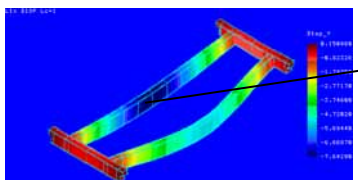
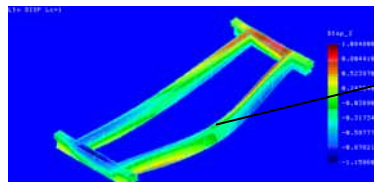
The analysis of the resistance structure of the crane bridge using finite elements have been calculated all the stresses and strains tensor from the structure nodes and from the centroids of the finite elements. In the post processing stage, for a quick and efficient interpretation of the results, there have been represented under the form of spectrum the tension fields at the whole structure level. Analyzing these data, it results a series of conclusions regarding the behavior of the resistance structure of the crane bridge. We have selected some values we have considered important from amongst the analysis of the folders which contained the results. This values are presented in table 1.

Table 1. Locating nodes which has the maximum tress value

No.	Analysis component	No. node which is recorded the extreme size	The extreme recorded size	The location of the node on the resistance structure of the crane bridge	Detail of the area which has extreme value
1.	$\sigma_x$	3123	132, 164 MPa		
		3080	-133, 064 MPa		
2.	$\sigma_y$	1702	- 182,226MPa		



No.	Analysis component	No. node which is recorded the extreme size	The extreme recorded size	The location of the node on the resistance structure of the crane bridge	Detail of the area which has extreme value
3.	$\sigma_z$	15 104	155,315 MPa		
4.	$\tau_{xy}$	1732	- 46, 996 MPa		
5.	$\tau_{zy}$	1809	30,73 MPa		
6.	$\tau_{zx}$	2517	- 76,85 MPa		
7.	$\sigma_{\text{von Mises}}$	15104	182,895 MPa		
8.	$\sigma_1$	15 104	182,89 MPa		
9.	$\sigma_2$	3132	81,92 MPa		

No.	Analysis component	No. node which is recorded the extreme size	The extreme recorded size	The location of the node on the resistance structure of the crane bridge	Detail of the area which has extreme value
10.	$\sigma_3$	1702	- 192,554 MPa		
11.	$u_{\max}$	15 991	20,1832 mm		node 15 991
12.	$v_{\min}$	7880	- 7,6429 mm		node 7880
13.	$w_{\min}$	15 343	-1,1586 mm		node 15 343

We have selected those values of the tension and deformation state which could cause some critical areas where stresses points are gathered (within the resistance structure of the crane bridge). We should consider that the beams of the strength structure of the crane bridge are made of OL 37 then, the analysis of stresses and strains is more effective if we use the theory of the specific form modifying energy (stated by von Misses) as a determining factor for reaching the limit stages, [13].

By analysing the tension fields, we are able to see the main critical area of the crane bridge. Thus, we have to pay all the attention while designing it as well as during the production, in case we want to redesign the resistance structure. The research performed allows the evaluation of the tensions state, pointing out the critical areas and measures which are imposed in order to increase the solidity and bearing capacity of the resistance structure for the crane bridge.

Analyzing the data presented in table 1, it

results a series of conclusions regarding the behavior of the resistance structure of the overhead crane bridge. The main conclusions which results from this analysis are:

a. The maximum equivalent tension calculated according to the theory of the specific form modifying energy (the theory of von Misses) is  $\sigma_{\text{von Misses}} = 182,895 \text{ MPa}$  and is recorded in the node 15104 placed in position No.7, on the lateral external surface of the longitudinal beam I near the connection with the right end beam. This size exceeds the allowable stress for case I of loading according to Bach, for the steel OL 37,  $\sigma_{\text{von Misses}} = 182,895 \text{ MPa} > \sigma_a$ , ( $\sigma_a = 150 \text{ MPa}$ ), with 21,92 %.

b. The maximum component in modulus of the tangential tension is the component  $\tau_{zx}$  which has the size  $|\tau_{zx}| = 76,85 \text{ MPa}$  and is recordered in the node 2517 placed in table 1, position No.6, at the upper part of the right end beam at the connection with the longitudinal beam I.



c. The components of the tangential stresses  $\tau_{xy}$  and  $\tau_{zy}$  recorded size in the nodes 1732 and 1809, as follows:  $\tau_{xy} = -46,996 \text{ MPa}$  and  $\tau_{zy} = 30,73 \text{ MPa}$ . These nodes are very closed and are placed according to table 1, positions 4 and 5 on the end of the right end beam near the origin of the global system of axes. In the same area, corresponding to the node 1702 is recorded the extreme value for the normal stress  $\sigma_y = -182,226 \text{ MPa}$  and the main normal stress with the size  $\sigma_3 = -192,554 \text{ MPa}$ .

d. According to the conclusions from point c, it results that the end beam area right placed near the origin of the global system of axes, is a critical area for which have to be taken measures of improving the constructive solution in order to decrease the peaks of tensions which appear. Similar situation appear according to conclusions from point a and b at the connection between the right beam and the longitudinal beam I.

e. As far as the main normal tensions are concerned -  $\sigma_1, \sigma_2, \sigma_3$  - they reach the highest values within the connection area between the two longitudinal beams and the right end beam, as follows:

- the main normal tension  $\sigma_1 = 182,89 \text{ N/mm}^2$ , reaches the highest value within the area which is close to the area where von Misses equivalent tension reaches the highest value, position No.8, table 1.

- the main normal tension  $\sigma_2 = 81,92 \text{ N/mm}^2$ , reaches the highest value within the area which is close to the highest point of the  $\sigma_1$  tension of the node 3123, position No.9, table 1.

- the main normal tension  $\sigma_3 = -192,554 \text{ N/mm}^2$ , reaches the highest value within the area which is close to the node 1702, position No.10, table 1.

f. The maximum total displacement is recorded in the node 15992, being of 20,87 mm, for which the linear displacement components according to the three directions of the global system of axes are:

$u = 15,18 \text{ mm}$ ,  $v = 3,75 \text{ mm}$ ,  $w = 0,075 \text{ mm}$ .

The extreme values of these components of displacements are recorded as follows:

$u_{\max} = 20,1832 \text{ mm}$  in node 15991;

$v_{\min} = -7,6429 \text{ mm}$  in node 7880;

$w_{\min} = -1,1586 \text{ mm}$  in node 15343, according to the location presented in table 1, positions 11, 12 and 13. These results are possible because the longitudinal beam I is twisted and bent and the shape of the cross section has been designed to take over the bending caused by the vertical loads. After we have analysed all the elements referring to the deformation, we concluded that

the longitudinal beam I represents the critical area for the resistance structure.

f. The complete study of the issue presented assumes an analysis of the structure behavior in dynamic conditions after the constructive solution improvement in order to reduce the peaks of stress.

## 6 Conclusions

All finite elements we have evaluated are used for shaping up the equipment, and they have ensured us a lot of possibilities for approximating the contour of the resistance structure, and we have distributed the tensions within the resistance structure of the crane bridge more appropriately.

The calculation pattern is effective due to the fact that we have used the appropriate finite elements for shaping up all the equipments, and the high quality of the elements is correlated to the required precision of the results of our study.

In order to establish the tensions and deformations of the resistance structure for a crane bridge with the help of finite elements, we had to establish the values of certain unknown functions. In our study, all tensions and deformations are well established. All features who have caused such tensions and deformations within the resistance structure of a crane bridge have been described mathematically, by differential equations, by integrating limit conditions specified by the analysis domain, and we have come up with some solutions to our problem. Due to the complexity of the resistance structure of a crane bridge, the loading conditions and the limit conditions, we have created a simple pattern of the structure (with finite elements), in order to solve the differential equations who describe all phenomena, and who cause the breaking out during tensions and deformations state of the resistance structure.

According to the results we have obtained, we can see that the calculation pattern had used the similar resistance structure of a crane bridge we are using nowadays.

The research performed allows the evaluation of the stress state, pointing out the critical areas and measures which are imposed in order to increase the solidity and bearing capacity of the strength structure for the rolling bridge.

By analysing the stresses fields, we are able to see that the main critical area of the rolling bridge is represented by the connection between the longitudinal beam I and the right-end beam. Also, the area of the right-end beam near the global axis system needs special attention in

order to improve the product and to eliminate any possible tension peak. Thus, we have to pay all the attention while designing it as well as during the production, in case we want to redesign the structure.

#### References

- [1] Alkin C., Imrak C.E., Kocabas H., Solid modelling and finite element analysis of an overhead crane bridge, *Acta Polytechnica*, Vol. 45, No. 3, 2005, pp. 61-67
- [2] Alkin C., Solid modelling of overhead crane bridges and analysis with finite element method, *M. Sc. Thesis*, Istanbul Technical University, Istanbul, Turkey, 2004
- [3] Banerje P.K., *The boundary element methods in engineering*, McGrawHill, 1994
- [4] Dumitru I., Faur N., *Calculation elements and application in the material strength*, Politechnica Publishing House, 1999
- [5] Errichello J., Crane design: Theory and calculations of reliability, *ASME Journal of Mechanical design*, Vol.105, 1983, pp. 283-284
- [6] Faur N., The evolution and calculation accuracy for the thin shell type finite element with moments, *Scientific Journal of University Politechnica of Timisoara*, Vol. 45(59), 2000, pp. 15-25
- [7] Ketill P., Willberger N.E, Application of 3D solid modelling and simulation programs to a bridge structure. *PhD. Thesis*, Chalmers University of Technology, Sweden
- [8] Mastorakis K., Martin O., Finite element modelling of filleted Structure, *Finite element method, published by WSEAS Press*, pp.38-43, 2008
- [9] Moustafa K.A., Abou-El-yazid T.G., Load Sway Control of overhauled cranes with load hoisting via stability analysis, *JSME Int. Journal*, Vol.39, Nr.1, 1996, pp.34-40.
- [10] Oltasen N.S., Petersson H. – *Introduction to the Finite Element Method*, Prentice-Hall, London, 1992
- [11] Pinca B. C., Optimization of a strength structure of a metallurgical aggregate, *PhD. Thesis*, Politechnica University, Timișoara, Romania, 2002
- [12] Stematiu D., *The calculus of the hidrotehnic structure*, Technical Publishing House, 1999
- [13] Timoshenko S., Gere J., *Theory of elastic stability*, Technical Publishing House, Bucharest, 1967
- [14] Zienkiewicz O.C, Taylor R. L., *La method des elements finis*, AFNOR, Paris, 1991
- [15] Yang Zun-hua, Jin Guang-zhen, 3DEFA analysis of metallurgy crane, *Journal of Hubei Politechnic University*, Vol.18, No.2, China, 2003
- [16] *COSMOS User's guide*, Structural research analysis corporation, Santa Monica, 1999